Evidence for the widespread occurrence of short- and medium-chain chlorinated paraffins in fish collected from the Rhône River basin (France)

Pierre Labadie, Charlotte Blasi, Karyn Le Menach, Emmanuel Geneste, Marc Babut, Olivier Perceval, Hélène Budzinski

Evidence for the widespread occurrence of short- and medium-chain chlorinated paraffins in fish collected from the Rhône River basin (France)

Pierre Labadie[a*], Charlotte Blasi[b], Karyn Le Menach[a], Emmanuel Geneste[b], Marc Babut[c], Olivier Perceval[d] and Hélène Budzinski[a]

[a]: CNRS, University of Bordeaux, EPOC, UMR 5805, F-33400 Talence, France

[b]: University of Bordeaux, CNRS, EPOC, UMR 5805, F-33400 Talence, France

[c]: UR RiverLY Irstea, F-69626 Villeurbanne cedex, France

[d]: French Agency for Biodiversity, 5 square Félix-Nadar, F-94300 Vincennes

*Contact author: pierre.labadie@u-bordeaux.fr, +33 (0)6 72 57 17 62

Published in Chemosphere, Volume 223, May 2019, Pages 232-239

https://doi.org/10.1016/j.chemosphere.2019.02.069

Abstract

Chlorinated paraffins (CPs) are high-volume chemicals used in numerous industrial applications. Their quantitative analysis is extremely challenging and this work presents the optimization of an analytical method based on gas chromatography hyphenated with electron capture negative ionization time-of-flight high-resolution mass spectrometry (GC-ECNI-TOF HRMS) for the simultaneous determination of short-chain and medium-chain CPs (SCCPs and MCCPs, respectively) in fish tissues (i.e. dorsal muscle). The resolution of the TOF-MS analyzer reduced or eliminated isobaric interferences and the CP response was optimized through Design of Experiment. A simple clean-up

procedure based on adsorption chromatography further removed some potentially interfering organochlorines. Good selectivity, linearity and accuracy were achieved; method detection limits or limits of reporting were compatible with expected levels in wild fish (0.03–0.35 ng g^{-1} wet weight, ww, depending on the congener). This method was proven suitable for the analysis of CPs in tissues of common barbel *Barbus barbus*, a fish species frequently used for water quality monitoring purposes in Europe. SCCPs and MCCPs were found to be widespread within the Rhône river basin (France). At all locations, MCCP concentrations (1.3 – 72.7 ng g^{-1} ww) were higher than those of SCCPs (0.3 – 10.6 ng g^{-1} ww) and levels were systematically lower than the proposed Predicted No Effect Concentrations (PNECs). Spatial variations of SCCP composition profiles largely surpassed those of MCCPs, suggesting the influence of local sources.

Keywords: chlorinated paraffins; time-of-flight mass spectrometry; river; fish; bioaccumulation

Highlights

1. GC-ECNI-TOF HRMS allowed for the quantitative analysis of SCCPs and MCCPs in fish

2. SCCPs and MCCPs were ubiquitous in the Rhône River basin

2. MCCP concentrations exceeded those of SCCPs at all locations

3. SCCP composition profile was variable, pointing to the influence of local sources

4. CP levels in fish were systematically lower than the proposed PNECs

1. Introduction

Chlorinated paraffins (CPs) are industrial chemicals produced by chlorination of n-alkane mixtures. Technical CP formulations contain thousands of isomers which degree of chlorination is usually between 40% and 70% Cl by weight and which carbon chain length is in the range C_{10}–C_{28} (Fiedler, 2010). Commercial mixtures can be divided into three groups: short-chain CPs (SCCPs, C_{10}–C_{13}), medium-chain CPs (MCCPs, C_{14}–C_{17}) and long-chain CPs (LCCPs, >C_{18}). CPs are used in a wide range of applications, e.g. as additives in metal working fluids, as plasticizers and as flame retardants in numerous polymeric products including plastics (mainly PVC) and rubbers (Fiedler, 2010). CPs are high-production volume chemicals, with a cumulative production higher than 7 million tons since 1930s, more than four times that of polychlorinated biphenyls (PCBs) (van Mourik et al., 2016).

SCCPs are considered as persistent in the environment and they have drawn increasing attention due to their toxic properties (El-Sayed Ali and Legler, 2010; POPRC, 2015). They have been detected in all environmental compartments, including humans and biota, and they may biomagnify in aquatic ecosystems (Houde et al., 2008a; Huang et al., 2017; Xia et al., 2017; Zhou et al., 2018). SCCPs were listed as Persistent Organic Pollutants and added to Annex A of the Stockholm Convention in 2017 (Glüge et al., 2018). They are expected to be replaced in numerous applications; production and use likely already shifted towards MCCPs prior to this classification (van Mourik et al., 2015). The persistence, bioaccumulation potential and toxicity of MCCPs have been less studied and the risk assessment of these chemicals is still ongoing (Glüge et al., 2018). Thus, there is still a need for additional knowledge on the occurrence and fate of CPs in the environment, especially for MCCPs (van Mourik et al., 2016).

The analysis of CPs in environmental matrices is extremely challenging due to the complexity of technical mixtures, variable composition of CP among samples, potential interference between CPs and from other organochlorines (van Mourik et al., 2015). Intercomparison studies demonstrated

large variations between laboratories (up to ten-fold), depending on the type of Mass Spectrometer (MS)and on the quantitation procedure (van Mourik et al., 2015; van Mourik et al., 2018). There is no consensus yet on analytical procedures for the determination of CPs in environmental samples and Sverko et al. (2012) highlighted the need to improve the quality of measurements to support global regulatory efforts. Early work was based on gas chromatography (GC) hyphenated with electron-capture negative ionization and low resolution mass spectrometry (GC/ECNI-LRMS), because it provides information on the CP chain length and degree of chlorination (Reth and Oehme, 2004; Reth et al., 2005b, a; Reth et al., 2006). This technique is, however, hampered by unresolvable interferences when operating at nominal mass. To overcome some of these limitations, Tomy et al. applied high-resolution mass spectrometry (ECNI-HRMS) using a magnetic sector analyzer for the analysis of SCCPs and MCCPs (Tomy et al., 1997; Tomy and Stern, 1999). Alternative quantification procedures were developed, based on multiple linear regression or multivariate analysis (Geiß et al., 2010; Nilsson et al., 2012). Recent work focused on the use of HRMS to improve the selectivity and the quantification performances for SCCPs and MCCPs, using for instance GC-Orbitrap-HRMS (Krätschmer et al., 2018). Time-of-flight (TOF) analyzers have also become available in numerous laboratories and have increasingly been used for the determination of CPs in environmental samples. Bogdal et al. (2015) developed a novel method based on chlorine-enhanced atmospheric pressure chemical ionization (APCI) with TOF-MS for fast CP quantitation in sewage sludge or urban air samples; this method was also used to quantify CPs in biota (Du et al., 2018). Huang et al. (2018) developed a fast screening method of SCCPs in indoor dust samples by graphene-assisted laser desorption/ionization TOF-MS. Two-dimensional gas-chromatography-ECNI-TOF was used for profiling and quantifying SCCPs and MCCPs in sediment and biological samples (Xia et al., 2016). Gao et al. (2016) explored the potential of one-dimensional GC-TOF-HRMS for the determination of CPs in a selection of matrices, including biological samples (e.g. vegetables); this technique, which is becoming increasingly available in analytical laboratories, gave promising results. Gao et al. (2016) recommended that further application of this method should be examined to achieve more accurate

analysis of CPs in environmental matrices. However, its capability to quantify CPs in biota samples has not been evaluated yet.

Thus, the objective of this study was two-fold. First, it aimed at examining the feasibility of quantifying SCCPs and MCCPs in complex fish muscle extracts using GC-ECNI-TOF-MS. The controlling factors of CP response in ECNI were explored using, for the first time, a chemometrics approach (i.e. Design of Experiment). Then, the second goal of this work was to apply this method, once optimized and validated, to the determination of SCCPs and MCCPs in fish samples collected at regional scale within the industrious Rhône River basin (France). This work thereby provides the first data at French national level and original data on the contamination of freshwater ecosystems by CPs.

2. Materials and methods

2.1. Chemicals and standards

C_{10}–C_{13} SCCP technical mixtures with chlorine content of 51.0, 55.5, and 63.0% (100 ng/µL in cyclohexane) and C_{14}–C_{17} MCCP mixtures with chlorine content of 42.0, 52.0 and 57.0% (100 ng/µL in cyclohexane) were purchased from Dr Ehrenstorfer (LGC, Molsheim, France). $^{13}C_{10}$-$C_{10}H_{16}Cl_6$ and $^{13}C_{10}$-syn-Dechlorane Plus (100 ng/µL in cyclohexane), both supplied by LGC, were used as surrogate and injection standard, respectively. Dichloromethane (DCM) was provided by Accros Organics (Noisy le Grand, France). Pentane was obtained from JT Baker (Atlantic Labo, Bruges, France) while sulfuric acid (Scharlau, 95-98% extra pure) and isooctane (Scharlau, HPLC Grade) were purchased from ICS (Gradignan, France). Silica gel (0.063-0.2 mm, Merck) was purchased from VWR International (Strasbourg, France) and cleaned-up with DCM prior to storage at 150 °C for activation. Acidified silica gel was obtained by mixing 60 g of silica gel and 40 g of sulfuric acid, following activation overnight at 200 °C. High purity gases were supplied by Linde (Saint Priest, France): nitrogen (4.5

grade), methane (4.5) and helium (6.0). Standard reference material (SRM) NIST 1974c (Organics in Mussel Tissue) was obtained from the National Institute of Standards and Technology (NIST) via LGC.

2.2. Sampling

Fish were collected from five water bodies selected within the Rhône River basin (France): Chéran river in Rumilly, Usses river in Seyssel, Combeauté river in Saint-Loup-Sur-Semouse, Rhône river in Tupins et Semons, Morge Canal in Poliénas (see Table S1 for geographic coordinates). These are all small rivers with mean flow rate in the range 2–8 $m^3 s^{-1}$, except the Rhône river which mean flow rate is much higher (1700 $m^3 s^{-1}$) (Banque Hydro).

The target species was the common barbel chub (*Barbel Barbel*), a cyprinid widely distributed in European freshwaters. Sampling was carried out between July 2009 and September 2009, except for the Rhône River where samples were taken in November 2011; a total of 22 samples were collected and treated as described below. At each site, three to five adult individuals (Table S1) were caught by electric fishing, anesthetized with eugenol, transported to the laboratory in a refrigerated cooler and kept at 4 °C until treatment within 24 hours of collection. Fish were measured (456 ± 74 mm, range: 370–560 mm), weighed (1116 ± 484 g, range: 480–1400 g, see SI for details) and dissected: the dorsal muscle was collected, frozen, freeze-dried and finely ground. Tissues were then stored at room temperature under controlled relative humidity.

2.3. Sample preparation

Freeze-dried muscle tissue (250–400 mg dry weight, dw) were spiked with $^{13}C_{10}$-$C_{10}H_{16}Cl_6$ (1.5 ng) and samples underwent microwave-assisted extraction in closed glass vessels with 10 mL of DCM, using a START E microwave system (Milestone SRL, Sorisole, Italy). Extraction time was set at 10 min: 5 min to reach the temperature set point (70 °C) followed by a 5-min holding time at 70 °C. Extracts were then filtered on glass fiber cotton, concentrated under a nitrogen stream to approximately 0.2

mL and solvent-exchanged to isooctane. A purification step was performed using bilayer columns consisting of 1 g of acidified silica gel and 1 g of activated silica gel (top to bottom), which were conditioned with 10 mL of pentane/DCM (9:1, v/v) followed by 10 mL of pentane. After extract loading, columns were rinsed with 10 mL of pentane (PCB-containing fraction, discarded) and CPs were eluted with 10 mL of pentane/DCM (9:1, v/v). Extracts were then concentrated under a nitrogen stream, transferred into an injection vial fitted with a 250 µL volume restrictor, together with 50 µL of isooctane. Finally, extracts were concentrated to a final volume of approximately 75 µL, spiked with the injection standard ($^{13}C_{10}$-syn-Dechlorane Plus, 1.5 ng) and stored at −20 ◦C until analysis. For each sample, the lipid content was estimated gravimetrically.

2.4. Analysis of SCCPs and MCCPs

CPs were analyzed by GC–MS using an Agilent 7890B GC system fitted with a J&W GC column (15 m x 0.25 mm id x 0.1 µm) and coupled to an Agilent 7200 Q-TOF analyzer. The system was controlled by Agilent MassHunter Acquisition software (version B.07.03.2129). It was operated in pulsed splitless injection mode (1.7 bar, 3 min) with an injector temperature of 225 ◦C. The helium carrier gas flow rate was 1.8 mL min^{-1} and the oven temperature program was as follows: 90 ◦C (1 min), 290 ◦C (28.5 ◦C min^{-1}) held for 4.5 min. The system was operated in electron capture negative chemical ionization (ECNI) using methane as reagent gas at a flow rate of 2 mL min^{-1}. Electron energy and emission current were set at 200 eV and 50 µA, respectively. The interface and source temperature were fixed at 290 and 150 ◦C, respectively.

The Q-ToF analyzer was operated in scan mode (i.e. TOF mode) at 5 spectra s^{-1}, over the m/z range 50–800. Tuning and calibration of the mass spectrometer was carried out with perfluorotributylamine to achieve a mass accuracy of <1 ppm. The analog to digital electronics sampling rate was set at 4 GHz, yielding a resolution of approximately 15,000 (FWHM) for m/z in the range 300–500 in profile mode. Acquisition was however performed in centroid mode so that file size

was kept <200 Mo, thereby allowing for peak integration and data export with the Agilent MassHunter Quantitative for TOF software (version B.07.01/Build 7.1.524.0). For all congener groups (i.e. $C_nH_{2n+2-x}Cl_x$), the most abundant and second most abundant peaks of the $[M-Cl]^-$ isotope cluster were used as the quantification and confirmation ions, respectively (Table S2 in the Supplementary MateriaI). The experimental isotope ratio, as determined using SCCP or MCCP standard solutions analyzed individually, was used to confirm the peak attribution to each congener group (margin applied : ±20%, although higher deviations could occasionally be observed for some low-intensity signals as reported by Krätschmer et al., 2018)). The mass extraction window was set at ±25 ppm for signal extraction from the total ion current signal. The m/z values monitored for $^{13}C_{10}$-$C_{10}H_{16}Cl_6$ and $^{13}C_{10}$-syn-Dechlorane Plus were $[M-Cl]^-$ and $[M]^-$, respectively.

The quantitation procedure was adapted from (Diefenbacher et al., 2015). Briefly, the response factor of SCCPs and MCCPs in a particular sample was estimated based on the chlorine content and the CP amount (ng) was determined using external calibration. Then, this amount was corrected for recoveries and for differences in extract volumes (details in the Supplementary MateriaI), and it was subsequently normalized to sample amount to calculate the CP concentration in fish muscle tissue (ng g^{-1}).

2.5. QA/QC

To minimize the risk of contamination, glassware was baked at 450 °C for 6 hours prior to its use. Procedural blanks consisting of 10 mL of DCM were analyzed for each sample batch; ∑SCCPs in the blanks were in the range 0.7 – 2.5 ng (1.6 ± 0.6 ng, n=9) while ∑MCCPs ranged from 0.7 to 1.6 ng (1.1 ± 0.3 ng, n=9, congener group pattern detailed in Tables S4 and S5). Blank correction was performed for the relevant congener groups. When analytes were detected in blanks, the Limit of Reporting (LoR) was defined as the standard deviation of blanks corrected by the $t_{n-1,95}$ Student coefficient, with n being the number of blank replicates (adapted from Bemrah et al., 2014). Otherwise, the Method

Detection Limit (MDL) was derived from the standard deviation of replicate measurements (n=7) performed on a low-contaminated fish muscle sample, (i.e. Thinlip mullet *Liza ramada* from the Gironde estuary, caught in 2012 (Munoz et al., 2017); SCCPs and MCCPs < 1 ng g^{-1} dw) fortified at 12.5 ng g^{-1} dw (i.e. approximately 3.1 ng g^{-1} ww) with standard mixtures of SCCP 63% Cl and MCCP 57% Cl. In this case, the MDL of each congener group was defined as the standard deviation of the concentration determined experimentally multiplied by $t_{n-1,99}$ (Muir and Sverko, 2006). Recovery rate and accuracy were determined on fish tissues fortified at 60 ng g^{-1} dw (i.e. 15 ng g^{-1} ww) with standard solutions of SCCP 63% Cl and MCCP 57% Cl. This spike level was deemed representative of levels expected in fish from the Rhône river basin. LORs, MDLs, recoveries and accuracy are discussed below in section 3.2.

2.6. Data analysis

The design of experiment (DOE) for ECNI optimization and the associated data analysis were performed using Minitab 17.2.1.0 (Minitab, Inc). This software was also used to perform analyses of variance (ANOVA) and covariance (ANCOVA); log-transformed data were used when the normality assumption was not met. Sigmaplot 12.5 was used to compute descriptive statistics, for linear regression and correlation analysis. Statistical significance was set at 0.05.

3. Results and discussion

3.1. GC-MS parameter optimization

To maximize analyte response, a short GC run was selected (< 12.5 min), in combination with high carrier gas flow rate, reduced column internal diameter and film thickness which allowed for narrowing chromatographic peaks. Inlet parameters had little effect on analyte response over the range 225–285 °C and the injection temperature was set at the lowest investigated value. Futhermore, a 4-factor/3-level Box-Behnken DOE was implemented to optimize source parameters through chemometrics, in order to explore the relative influence of potential key factors but also to investigate whether there were significant interactions between these factors. This approach was introduced in order to limit the number of analyses and the primary advantage of the Box-Behnken DOE is addressing the issue of experimental boundaries, especially to avoid extreme combinations of factors (Miller and Miller, 2010). The investigated variables were as follows: reagent gas flow rate (2–3mL min^{-1}), source temperature (150–200 °C), electron energy (150-200 eV) and emission current (50–150 μA). Source temperature was investigated over a limited range, avoiding temperature >200°C, so as to minimize SCCP and MCCP fragmentation (Tomy et al., 1997). Contrary to findings by Gao et al. (2016) who used the same ECNI-TOF apparatus, this parameter was found to have very little effect on analyte response (based on the signal to noise ratio, S/N). It was therefore set at the lowest value (150 °C) to minimize fragmentation (Tomy et al., 1997), thereby simplifying mass spectra and reducing the risk of self-interferences between CPs (Krätschmer et al., 2018). For instance, beside $[Cl_2]^-$, $[M\text{-}Cl]^-$ and, to a lesser extent, $[M\text{-}HCl]^-$ were the only ions observed in the mass spectrum of $^{13}C_{10}$-$C_{10}H_{16}Cl_6$ (Figure S2). Similarly, the reagent flow rate did not significantly affect analyte S/N ratio and it was thus also set at the lowest investigated value (2 mL min^{-1}) to save methane. Electron energy appeared to be the most influential parameter, while low but significant influence of the emission current was also observed. Furthermore, data analysis revealed a weak but

significant interaction between electron energy and emission current; this interaction was however relatively stable over the whole range of electron energy and emission current investigated values. Figure 1 illustrate these results for $C_{12}H_{19}Cl_7$ only but similar conclusions could be drawn for the other homologue (same chain length but different chlorine number) and chain length groups (same chain length but different chlorine number) (data not shown). The largest S/N was observed for a combination of the highest electron energy and emission current values (Figure 2), and such settings could be used in order to maximize analyte response. However, extreme settings were avoided to promote the robustness of routine analyses: emission current was thus set at 50 µA (setting recommended by the manufacturer) while electron energy was set at 200 eV. With these settings, the S/N was only reduced by less than a factor 2 compared to the maximum value (Figure 2).

Under such conditions, instrument detection limits (IDLs) were determined by replicating five analyses of technical SCCP and MCCP standard solutions. For each congener group, the IDL was calculated by multiplying the standard deviation of the signal intensity by the Student's t-value at a 99% confidence level (one-tailed) (Bogdal et al., 2015). IDLs were in the range 0.2 – 6 pg injected for the different congener groups present in the standard mixtures and compared well with previous data acquired using GC-TOF-MS (Gao et al., 2016) or HPLC-APCI-HRMS (Bogdal et al., 2015). In the present work, the TOF analyzer was operated in high-resolution mode, with a supposedly narrower dynamic range than when operated at lower resolution. To test the linearity of the response, 7-point curves covering the range 200 pg – 600 ng injected on column (i.e. for ∑SCCPs or ∑MCCPs) were fitted using standard solutions. The linearity range spanned more than three decades (Figure S3), in good agreement with (Gao et al., 2016). These findings confirm that this TOF instrument was suitable for the quantitative analysis of CPs at levels expected in environmental samples.

3.2. Method performance

The TOF-MS was operated at resolution of 15000 FWHM, which is sufficient to resolve all SCCP and MCCP congener groups and to eliminate self-interferences between SCCPs and MCCPs as long as only the two most abundant isotope peaks of the $[M\text{-}Cl]^-$ cluster are considered (Gao et al., 2016; Krätschmer et al., 2018). Organochlorines such as PCBs may also interfere with some SCCPs (e.g. hexa-CBs, $C_{12}H_4Cl_6$, vs $[M\text{-}Cl]^-$ of $C_{11}H_{17}Cl_7$, Δm= 98 mDa); such isobaric interferences were largely removed by to the resolution of the TOF analyzer (Figure S4). To further eliminate the risk of interferences, a clean-up procedure was implemented with bilayer columns consisting of H_2SO_4-impregnated silica gel and activated silica gel. The aim of this procedure was two-fold: *i)* separation or elimination of potentially interfering organochlorines from CPs and *ii)* elimination of matrix components that may alter the robustness of the GC-MS analysis. For instance, the use of activated silica gel enabled the complete separation of PCBs from CPs and thus eliminated PCB isobaric interferences in fish extracts (Figure S5). In addition, activated silica in combination with H_2SO_4-impregnated silica gel is also known to completely or partially separate CPs from numerous organochlorines potentially interfering with SCCP determination, e.g. dieldrin or toxaphenes (Chen et al., 2013). This sorbent also efficiently removes matrix components such as triglycerides, providing cleaner extracts and thereby minimizing GC artefacts such as retention time drift or loss of sensitivity due to source fouling (Labadie et al., 2010). The clean-up efficiency was highlighted by the fact that no significant loss of signal was observed for neither SCCPs nor MCCPs when analyzing series consisting of approximately 25 fish extracts; since quantitation was performed by external calibration, this proved essential to ensure satisfactory performances for large samples batches.

MDLs/LoRs were in the range 0.04–0.2 ng g^{-1} wet weight (ww) (i.e. 3 – 19 ng g^{-1} lipid weight, lw) for the different SCCP congener groups and in the range 0.05–0.4 ng g^{-1} ww (i.e. 4 – 28 ng g^{-1} lw) for MCCPs, in the same range than those obtained previously using magnetic sector HRMS (Houde et al., 2008a). Detailed values of MDLs/LoRs expressed on ww, lw and dw basis are given in Table S2.

Recovery rates were in the range 103 ± 7% and 85 ± 10% for ∑SCCPs and ∑MCCPs, respectively, while that of the ^{13}C-labeled surrogate was estimated at 81 ± 13%. Accuracy, as determined on samples fortified with both analytes and surrogate prior to the extraction step, was satisfactory since repeatability was 85 ± 5% and 83 ± 6% for ∑SCCPs and ∑MCCPs, respectively (n=6). In addition, reproducibility was 85 ± 11% and 93 ± 13% for ∑SCCPs and ∑MCCPs, respectively (n=10).

The quantification procedure was further validated by analyzing NIST 1974c SRM, which had been previously used by others for intra-laboratory controls (Houde et al., 2008b; Saborido Basconcillo et al., 2015). In the present work, it was determined that this SRM contained 12.5 ± 1.5 ng/g ww (n=5) of ∑SCCPs and 23.1 ± 3.7 ng/g ww (n=6) of ∑MCCPs. Such results are in close agreement with those previously reported using magnetic sector HRMS (Figure S6). Furthermore, the method quantification performance was further tested within the frame of a QUASIMEME interlaboratory study on the analysis of SCCPs in environmental matrices (QUASIMEME). Satisfactory results (i.e. z-score < 2) were achieved for fish extracts (European eel, *Anguilla anguilla*; van Mourik et al., 2018).

3.3. Concentrations of SCCPs and MCCPs

In this study, CPs were analyzed for the first time in fish collected from European continental water bodies. The detection frequency of SCCPs and MCCPs was 100%, thereby indicating the ubiquity of these chemicals in fish from the Rhône river basin. Overall, total SCCP concentrations were in the range 0.3 – 10.6 ng g^{-1} ww (i.e. 63 – 1492 ng g^{-1} lw) (Figure 3 and Table S1) and they were systematically two to three orders of magnitude lower than the predicted no-effect concentration (PNEC) (e.g. toxicity threshold associated with secondary poisoning) proposed for ∑SCCPs: 5.5 µg g^{-1} ww (Pakalin et al., 2008). When considering all locations, the median concentration of ∑SCCPs was 3.6 ng g^{-1} ww (i.e. 728 ng g^{-1} lw). Recent reports on SCCP and MCCP concentrations in biological samples focused on aquatic biota (e.g. fish and macroinvertebrates), mainly collected from North

America and China (van Mourik et al., 2016). Large differences were observed between studies, which may partly be due to analytical issues (van Mourik et al., 2015). Nevertheless, the levels observed in the present work are in the same order of magnitude than those reported for lake trout (*Salvelinus namaycush*) in the Great Lakes (12 – 288 ng g^{-1} lw) (Saborido Basconcillo et al., 2015), polar cod (*Boreogadus saida*) in the Norwegian Arctic (134 ng g^{-1} lw) (Herzke et al., 2013), or several fish species from the Ebro Delta in Spain (3–141 ng g^{-1} ww) (Parera et al., 2013). Regardless of the mode of expression of SCCP concentrations, (i.e. ng g^{-1} ww or ng g^{-1} lw), no significant differences could be observed between the sites investigated in the present study. This was possibly due to high interindividual variability, as observed in other fish species (Huang et al., 2017), and to the low number of individuals collected at some sites (e.g. n=3 for the Morge Canal).

In the present study, when considering all locations, ∑MCCPs was in the range 1.3 – 72.7 ng g^{-1} ww (i.e. 99 – 11300 ng g^{-1} lw) (Figure 3 and Table S1), while the median ∑MCCPs concentration was 18.5 ng g^{-1} ww (i.e. 4430 ng g^{-1} lw) (Figure 3). Fish collected from the Chéran and Combeauté rivers displayed significantly higher ∑MCCP concentrations than those observed in the Rhône River, but did not exceed a recently proposed PNEC (11 ng g^{-1} ww whole fish) (Glüge et al., 2018). Such levels are much higher than those reported for lake trout from the Great Lakes (13 – 130 ng g^{-1} lw) (Saborido Basconcillo et al., 2015) or polar cod from Norway (89 ng g^{-1} lw). They are, however, comparable with those recently reported for various fish species at Liaodong Bay, North China (22 – 5097 ng g^{-1} lw), which were among the highest reported in the literature (Huang et al., 2017).

A weak but significant correlation between total concentrations of MCCPs and SCCPs was observed when considering the whole dataset (Figure S7). Discrepancies were, however, observed between sites: while strong correlations were reported for the Rhône and Chéran rivers ($R^2 > 0.90$), no significant correlation was observed at the other sites. This suggests that the exposure of fish to CPs might partly be controlled by local contamination sources (see section 3.4), although diet composition may also be at play.

Total MCCP levels were systematically higher than those of SCCPs and the concentration ratio ranged from 2 to 55 (median: 5.6). Site-specific particularities were observed: for instance, the Rhône river exhibited significantly lower MCCPs to SCCPs ratios than the Chéran or Usses rivers. Contrasted situations were also observed in Canada where freshwater fish from the most industrialized and populated areas contained higher levels of MCCPs than SCCPs, whereas fish from more remote sites displayed higher SCCP to MCCP ratios (Saborido Basconcillo et al., 2015). A pattern consistent with these observations was reported in polar cod in the Norwegian Arctic, where SCCPs concentrations were higher than those of MCCPs (Herzke et al., 2013). Huang et al. (2017) reported similar results for most fish species from the coastal environment of Liaodong Bay, North China. The higher MCCP to SCCP ratios observed at our study sites was possibly due to the influence of local CP sources relative to atmospheric deposition, although it may also reflect the industrial shift to MCCPs in recent years (de Boer, 2010). Site-specific MCCP to SCCP ratios may be attributed to local variations over time of the relative influence of SCCP and MCCP sources, resulting in locally and temporally varying CP patterns for different water bodies.

In this study, SCCP and MCCP concentrations displayed large interindividual variability in fish at all locations, e.g. relative standard deviation in the range 41–123% and 42–117% for SCCPs and MCCPs, respectively. To further investigate the determinants of SCCP and MCCP bioaccumulation in *B. barbus* from the Rhône river catchment, an ANCOVA was performed on ∑SCCPs and ∑MCCPs (ww basis) with site and sex as qualitative variables and length, weight and lipid as quantitative variables. None of these factors proved significant as previously observed for other fish species and sampling locations, indicating that the influence of biological factors on CP accumulation remains unclear as already pointed out by van Mourik et al. (2016).

3.4. CP homologue and chain length group patterns

Saborido Basconcillo et al. (2015) reported that the congener group pattern of SCCPs in fish differed between freshwater systems in Canada (e.g. Lake Huron vs Lake Superior and Lake Erie), depending on the relative influence of atmospheric deposition and local urban or industrial sources. For instance, shorter-chain ($<C_{11}$) and lower chlorinated SCCPs are more volatile and exhibit long atmospheric lifetimes, which facilitates their transport to remote locations (van Mourik et al., 2016). Overall, the SCPP pattern observed in barbel tissues from the Rhône river basin appeared to be dominated by longer-chained congener groups (Table S4), with higher chlorine atom numbers than in recent reports focusing on biota from China (Huang et al., 2017; Zhou et al., 2018). An ANCOVA analysis performed on the SCCP pattern showed that site was the only significant factor (data not shown). Thus, the spatial variability of the SCCP relative abundance was investigated using hierarchical ascendant classification (Figure S8). Using a similarity threshold of 50%, two groups could be distinguished: the first group comprised all fish from the Rhône river and the Morge Canal and most individuals from the Usses and Chéran rivers. The second group consisted essentially of fish from the Combeauté river and it was characterized by *i)* significantly higher relative abundance of C_{12} and C_{13} SCCPs and *ii)* significantly lower abundance of C_{10} and C_{11} compounds. The largest pattern differences were actually observed between the Rhône and Combeauté rivers (Figure 4). In the Rhône river, C_{11} and C_{12} congener groups were predominant, especially $C_{11}H_{17}Cl_7$ (8.5 ± 3.7%), $C_{11}H_{16}Cl_8$ (9.3 ± 1.5%), $C_{11}H_{15}Cl_9$ (8.1 ± 1.6%), $C_{12}H_{18}Cl_8$ (7.9 ± 1.2%), $C_{12}H_{17}Cl_9$ (9.7 ± 1.8%) and $C_{12}H_{16}Cl_{10}$ (7.8 ± 1.5%). The overall prevalence of octa- to nona-chlorinated compounds was also observed in salmonids from Lake Huron (Saborido Basconcillo et al., 2015). In contrast, the SCCP pattern in fish from the Combeauté river was characterized by longer chain groups and higher-chlorinated homologues, i.e. $C_{12}H_{17}Cl_9$ (9.7 ± 1.0%), $C_{12}H_{16}Cl_{10}$ (16.7 ± 3.3%), $C_{13}H_{19}Cl_9$ (12.7 ± 0.7%) and $C_{13}H_{18}Cl_{10}$ (12.5 ± 3.5%). Wang et al. (2013) showed that congeners with high number of carbon or chlorine atoms (e.g. C_{12}-C_{13} and Cl_8–C_{10}) were more prevalent in soil samples collected near urban or industrial areas. Similar patterns were observed in fish and macroinvertebrates collected from the

Pearl River estuary in China, subjected to fast industrialization and urbanization as well as e-waste recycling activities (Sun et al., 2016). Wood processing might a significant source of SCCPs (de Boer, 2010) and several sawmill and wood panel factories are located within the watershed of the Combeauté river. Therefore, it cannot be excluded that the specific pattern observed in fish from this water body is associated with such industrial activities. It should also be noted that factors not considered in the present work such as fish age or prey specific to each river system may also have influenced the observed SCCP patterns.

Contrary to SCCPs, the homologue patterns of MCCPs appeared to be fairly homogenous and no significant difference was observed between sites. At all locations, C_{14} congeners were dominant and accounted on average for 38–51% of ∑MCCPs (Table S5). $C_{14}H_{23}Cl_7$, $C_{14}H_{22}Cl_8$ and $C_{14}H_{21}Cl_9$ were usually the prevailing compounds but $C_{14}H_{20}Cl_{10}$ was also observed, especially in the Rhône and Combeauté rivers (Figure 4). C_{15} congener groups were less abundant but contributed on average to 23–27% of ∑MCCPs (Table S5). These findings are consistent with the fact that the contamination of aquatic biota worldwide appear to be clearly dominated by MCCPs with 14 carbon atoms (van Mourik et al., 2016). For instance, Houde et al. (2008) observed that $C_{14}H_{22}Cl_8$ was the most abundant group in Lake Ontario lake trout and Saborido-Basconcillo et al. (2015) found that $C_{14}H_{23}Cl_7$, $C_{14}H_{22}Cl_8$ and $C_{14}H_{21}Cl_9$ were abundant groups in salmonids collected from lakes in more industrialized and urbanized areas. Reports for fish collected from Liaodong Bay (China) also indicated that C_{14} MCCPs were the dominating group in all investigated fish species, accounting for 61–97% of ∑MCCPs while C_{15} MCCPs were the second most abundant group (7–24%), followed by C_{16} and C_{17} MCCPs (Huang et al., 2017). Recently, Krätschmer et al. (2018) also observed the predominance of C_{14} MCCPs over C_{15}-C_{17} congeners in farmed salmon (*Salmo salar*) from Norway.

4. Conclusions

This work reported on the optimization of a GC-ECNI-TOF method for the determination of SCCPs and MCCPs in fish tissues. The resolution of the TOF-MS reduced or eliminated isobaric interferences and the CP response was optimized through DOE. This method proved suitable for the analysis of CPs in the tissues of the common barbel *B. barbus*. This work provides original data on the contamination of selected French freshwater bodies by SCCPs and MCCPs prior to the listing of SCCPs in the Stockholm Convention on POPs; both groups appeared to be widespread within the industrious Rhône river basin. MCCP concentrations were higher than those of SCCPs at all locations and these levels were systematically lower than the proposed PNECs. Spatial variations of SCCP composition profile largely surpassed those of MCCPs, suggesting the influence of local sources. Additional research is needed to gain further insight into the factors controlling the bioaccumulation of SCCP and MCCPs in aquatic biota, while investigating time trends (e.g. using sediment cores) would provide valuable information to assess past exposure to CPs.

Acknowledgements

This study was funded by the French National Agency for Biodiversity (AFB). The Aquitaine Region and the European Union (CPER A2E project) are acknowledged for their financial support. This study also benefitted from grants from the French National Research Agency (ANR) as part of the Investments for the Future Program (Cluster of Excellence COTE, ANR-10-LABX-45).

References

Bemrah, N., Jean, J., Rivière, G., Sanaa, M., Leconte, S., Bachelot, M., Deceuninck, Y., Bizec, B.L., Dauchy, X., Roudot, A.-C., Camel, V., Grob, K., Feidt, C., Picard-Hagen, N., Badot, P.-M., Foures, F., Leblanc, J.-C., 2014. Assessment of dietary exposure to bisphenol A in the French population with a special focus on risk characterisation for pregnant French women. Food Chem. Toxicol. 72, 90-97.

Bogdal, C., Alsberg, T., Diefenbacher, P.S., MacLeod, M., Berger, U., 2015. Fast Quantification of Chlorinated Paraffins in Environmental Samples by Direct Injection High-Resolution Mass Spectrometry with Pattern Deconvolution. Anal. Chem. 87, 2852-2860.

Chen, L., Huang, Y., Han, S., Feng, Y., Jiang, G., Tang, C., Ye, Z., Zhan, W., Liu, M., Zhang, S., 2013. Sample pretreatment optimization for the analysis of short chain chlorinated paraffins in soil with gas chromatography–electron capture negative ion-mass spectrometry. J. Chrom. A 1274, 36-43.

de Boer, J., 2010. Chlorinated Paraffins, The Handbook of Environmental Chemistry, Vol. 10. Springer Berlin Heidelberg.

Diefenbacher, P.S., Bogdal, C., Gerecke, A.C., Glüge, J., Schmid, P., Scheringer, M., Hungerbühler, K., 2015. Short-Chain Chlorinated Paraffins in Zurich, Switzerland—Atmospheric Concentrations and Emissions. Environ. Sci. Technol. 49, 9778-9786.

Du, X., Yuan, B., Zhou, Y., Benskin, J.P., Qiu, Y., Yin, G., Zhao, J., 2018. Short-, Medium-, and Long-Chain Chlorinated Paraffins in Wildlife from Paddy Fields in the Yangtze River Delta. Environ. Sci. Technol. 52, 1072-1080.

El-Sayed Ali, T., Legler, J., 2010. in de Boer, Chlorinated Paraffins, The Handbook of Environmental Chemistry, Vol. 10. Springer Berlin Heidelberg.

Fiedler, H., 2010. in de Boer, Chlorinated Paraffins, The Handbook of Environmental Chemistry, Vol. 10. Springer Berlin Heidelberg.

Gao, W., Wu, J., Wang, Y., Jiang, G., 2016. Quantification of short- and medium-chain chlorinated paraffins in environmental samples by gas chromatography quadrupole time-of-flight mass spectrometry. J Chromatogr A 24, 98-106.

Geiß, S., Einax, J.W., Scott, S.P., 2010. Determination of the Sum of Short Chain Polychlorinated n-Alkanes with a Chlorine Content of Between 49 and 67% in Water by GC-ECNI-MS and Quantification by Multiple Linear Regression. Clean Soil, Air, Water 38, 57-76.

Glüge, J., Schinkel, L., Hungerbühler, K., Cariou, R., Bogdal, C., 2018. Environmental Risks of Medium-Chain Chlorinated Paraffins (MCCPs): A Review. Environ. Sci. Technol. 52, 6743-6760.

Herzke, D., Kaasa, H., Gravem, F., Gregersen, H., Jensen, J.B., Horn, J., Harju, M., Borgen, A., Enge, E., Warner, N., 2013. Perfluorinated alkylated substances, brominated flame retardants and chlorinated paraffins in the Norwegian Environment-screening 2013. Norwegian Environment Agency. NILU–Norsk Institutt for Luftforskning. SWECO, Tromsø, Norway.

Houde, M., Muir, D.C., Tomy, G.T., Whittle, D.M., Teixeira, C., Moore, S., 2008. Bioaccumulation and trophic magnification of short- and medium-chain chlorinated paraffins in food webs from Lake Ontario and Lake Michigan. Environ. Sci. Technol. 42, 3893-3899.

Huang, H., Gao, L., Xia, D., Qiao, L., 2017. Bioaccumulation and biomagnification of short and medium chain polychlorinated paraffins in different species of fish from Liaodong Bay, North China. Scientific Reports 7, 10749.

Huang, X., Liu, Q., Gao, W., Wang, Y., Nie, Z., Yao, S., Jiang, G., 2018. Fast screening of short-chain chlorinated paraffins in indoor dust samples by graphene-assisted laser desorption/ionization mass spectrometry. Talanta 179, 575-582.

Banque Hydro, http://www.hydro.eaufrance.fr/.

Krätschmer, K., Cojocariu, C., Schächtele, A., Malisch, R., Vetter, W., 2018. Chlorinated paraffin analysis by gas chromatography Orbitrap high-resolution mass spectrometry: Method performance, investigation of possible interferences and analysis of fish samples. J. Chrom. A 1539, 53-61.

Labadie, P., Alliot, F., Bourges, C., Desportes, A., Chevreuil, M., 2010. Determination of polybrominated diphenyl ethers in fish tissues by matrix solid-phase dispersion and gas chromatography coupled to triple quadrupole mass spectrometry: Case study on European eel (Anguilla anguilla) from Mediterranean coastal lagoons. Anal. Chim. Acta 675, 97-105.

Miller, J.N., Miller, J.C., 2010. Statistics and chemometrics for analytical chemistry, 6th ed ed. Prentice Hall, Harlow.

Muir, D., Sverko, E., 2006. Analytical methods for PCBs and organochlorine pesticides in environmental monitoring and surveillance: a critical appraisal. Anal. Bioanal. Chem. 386, 769-789.

Munoz, G., H. Budzinski, M. Babut, H. Drouineau, M. Lauzent, K.L. Menach, J. Lobry, J. Selleslagh, C. Simonnet-Laprade, et P. Labadie. 2017. Evidence for the Trophic Transfer of Perfluoroalkylated Substances in a Temperate Macrotidal Estuary. Environ. Sci. Technol. 51, 8450-59.

Nilsson, M.-L., Bengtsson, S., Kylin, H., 2012. Identification and determination of chlorinated paraffins using multivariate evaluation of gas chromatographic data. Environ. Pollut. 163, 142-148.

Pakalin, S., Aschberger, K., Cosgrove, O., Paya-Perez, A., Vegro, S., 2008. European Union Risk Assessment Report, Alkanes, C10-13, chloro, Volume 81. European Commission. OPOCE, ISSN:1018-5593, EUR 23396 EN, available online at https://ec.europa.eu/jrc/en/publication/eur-scientific-and-technical-research-reports/updated-european-union-risk-assessment-report-alkanes-c10-13-chloro.

Parera, J., Ábalos, M., Santos, F.J., Galceran, M.T., Abad, E., 2013. Polychlorinated dibenzo-p-dioxins, dibenzofurans, biphenyls, paraffins and polybrominated diphenyl ethers in marine fish species from Ebro River Delta (Spain). Chemosphere 93, 499-505.

POPRC, 2015. Short-chained Chlorinated Paraffins: Risk Profile Document UNEP/POPS/POPRC.11/10/Add.2. United Nations Environmental Programme Stockholm Convention on Persistent Organic Pollutants, Geneva. http://chm.pops.int/Portals/0/download.aspx?d=UNEP-POPS-POPRC.12-11-Add.3.English.pdf.

QUASIMEME, http://www.quasimeme.org., last accessed on 7th February 2019.

Reth, M., Ciric, A., Christensen, G.N., Heimstad, E.S., Oehme, M., 2006. Short- and medium-chain chlorinated paraffins in biota from the European Arctic — differences in homologue group patterns. Sci. Total Environ. 367, 252-260.

Reth, M., Oehme, M., 2004. Limitations of low resolution mass spectrometry in the electron capture negative ionization mode for the analysis of short- and medium-chain chlorinated paraffins. Anal. Bioanal. Chem. 378, 1741-1747.

Reth, M., Zencak, Z., Oehme, M., 2005a. First study of congener group patterns and concentrations of short- and medium-chain chlorinated paraffins in fish from the North and Baltic Sea. Chemosphere 58, 847-854.

Reth, M., Zencak, Z., Oehme, M., 2005b. New quantification procedure for the analysis of chlorinated paraffins using electron capture negative ionization mass spectrometry. J. Chrom. A 1081, 225-231.

Saborido Basconcillo, L., Backus, S.M., McGoldrick, D.J., Zaruk, D., Sverko, E., Muir, D.C., 2015. Current status of short- and medium chain polychlorinated n-alkanes in top predatory fish across Canada. Chemosphere 127, 93-100.

Sun, R., Luo, X., Tang, B., Li, Z., Huang, L., Wang, T., Mai, B., 2016. Short-chain chlorinated paraffins in marine organisms from the Pearl River Estuary in South China: Residue levels and interspecies differences. Sci. Total Environ. 553, 196-203.

Sverko, E., Tomy, G.T., Märvin, C.H., Muir, D.C.G., 2012. Improving the Quality of Environmental Measurements on Short Chain Chlorinated Paraffins to Support Global Regulatory Efforts. Environ. Sci. Technol. 46, 4697-4698.

Tomy, G.T., Stern, G.A., 1999. Analysis of C(14)-C(17) Polychloro-n-alkanes in Environmental Matrixes by Accelerated Solvent Extraction-High-Resolution Gas Chromatography/Electron Capture Negative Ion High-Resolution Mass Spectrometry. Anal. Chem. 71, 4860-4865.

Tomy, G.T., Stern, G.A., Muir, D.C.G., Fisk, A.T., Cymbalisty, C.D., Westmore, J.B., 1997. Quantifying C10−C13 Polychloroalkanes in Environmental Samples by High-Resolution Gas Chromatography/Electron Capture Negative Ion High-Resolution Mass Spectrometry. Anal. Chem. 69, 2762-2771.

van Mourik, L.M., Gaus, C., Leonards, P.E.G., de Boer, J., 2016. Chlorinated paraffins in the environment: A review on their production, fate, levels and trends between 2010 and 2015. Chemosphere 155, 415-428.

van Mourik, L.M., Leonards, P.E.G., Gaus, C., de Boer, J., 2015. Recent developments in capabilities for analysing chlorinated paraffins in environmental matrices: A review. Chemosphere 136, 259-272.

van Mourik, L.M., van der Veen, I., Crum, S., de Boer, J., 2018. Developments and interlaboratory study of the analysis of short-chain chlorinated paraffins. TrAC, Trends Anal. Chem. 102, 32-40.

Wang, Y., Li, J., Cheng, Z., Li, Q., Pan, X., Zhang, R., Liu, D., Luo, C., Liu, X., Katsoyiannis, A., Zhang, G., 2013. Short- and Medium-Chain Chlorinated Paraffins in Air and Soil of Subtropical Terrestrial Environment in the Pearl River Delta, South China: Distribution, Composition, Atmospheric Deposition Fluxes, and Environmental Fate. Environ. Sci. Technol. 47, 2679-2687.

Xia, D., Gao, L., Zheng, M., Li, J., Zhang, L., Wu, Y., Tian, Q., Huang, H., Qiao, L., 2017. Human Exposure to Short- and Medium-Chain Chlorinated Paraffins via Mothers' Milk in Chinese Urban Population. Environ. Sci. Technol. 51, 608-615.

Xia, D., Gao, L., Zheng, M., Tian, Q., Huang, H., Qiao, L., 2016. A Novel Method for Profiling and Quantifying Short- and Medium-Chain Chlorinated Paraffins in Environmental Samples Using Comprehensive Two-Dimensional Gas Chromatography–Electron Capture Negative Ionization High-Resolution Time-of-Flight Mass Spectrometry. Environ. Sci. Technol. 50, 7601-7609.

Zhou, Y., Yin, G., Du, X., Xu, M., Qiu, Y., Ahlqvist, P., Chen, Q., Zhao, J., 2018. Short-chain chlorinated paraffins (SCCPs) in a freshwater food web from Dianshan Lake: Occurrence level, congener pattern and trophic transfer. Sci. Total Environ. 615, 1010-1018.

List of figures

Figure 3. Total concentrations of SCCPs (top) and MCCPs (bottom) in individual common barbel collected from selected locations in the Rhône River watershed. ww: wet weight / lw: lipid weight

Figure 4. Average SCCP and MCCP congener group pattern in common barbel collected from the Combeauté River (left) and Rhône River (right). Error bars represent the standard deviation (n=4 and 5 for the Combeauté River and Rhône River, respectively).

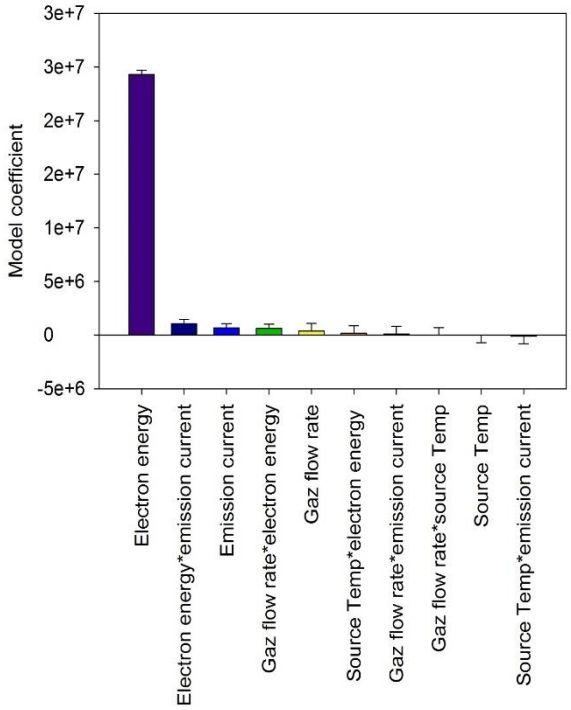

Figure 1. Pareto chart of the standardized effects of ECNI parameters (example of $C_{12}H_{19}Cl_7$).

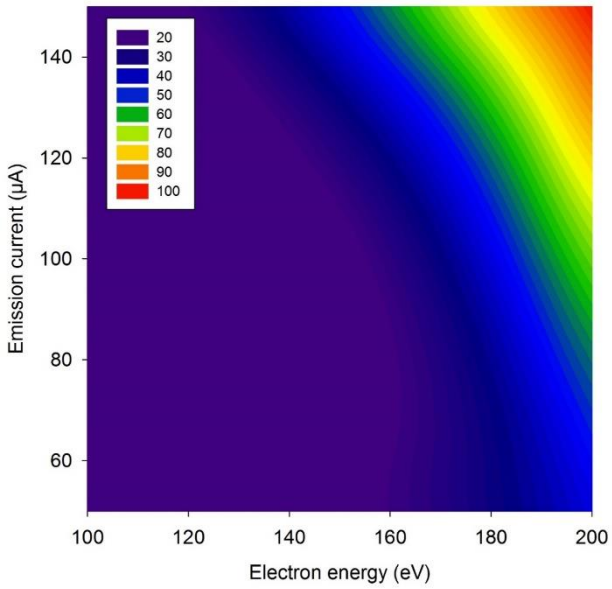

Figure 2. Relative response surface for $C_{12}H_{19}Cl_7$, as a function of emission current and electron energy (gas flow rate set at 2.5 mL min^{-1} and source temperature set at 175°C).

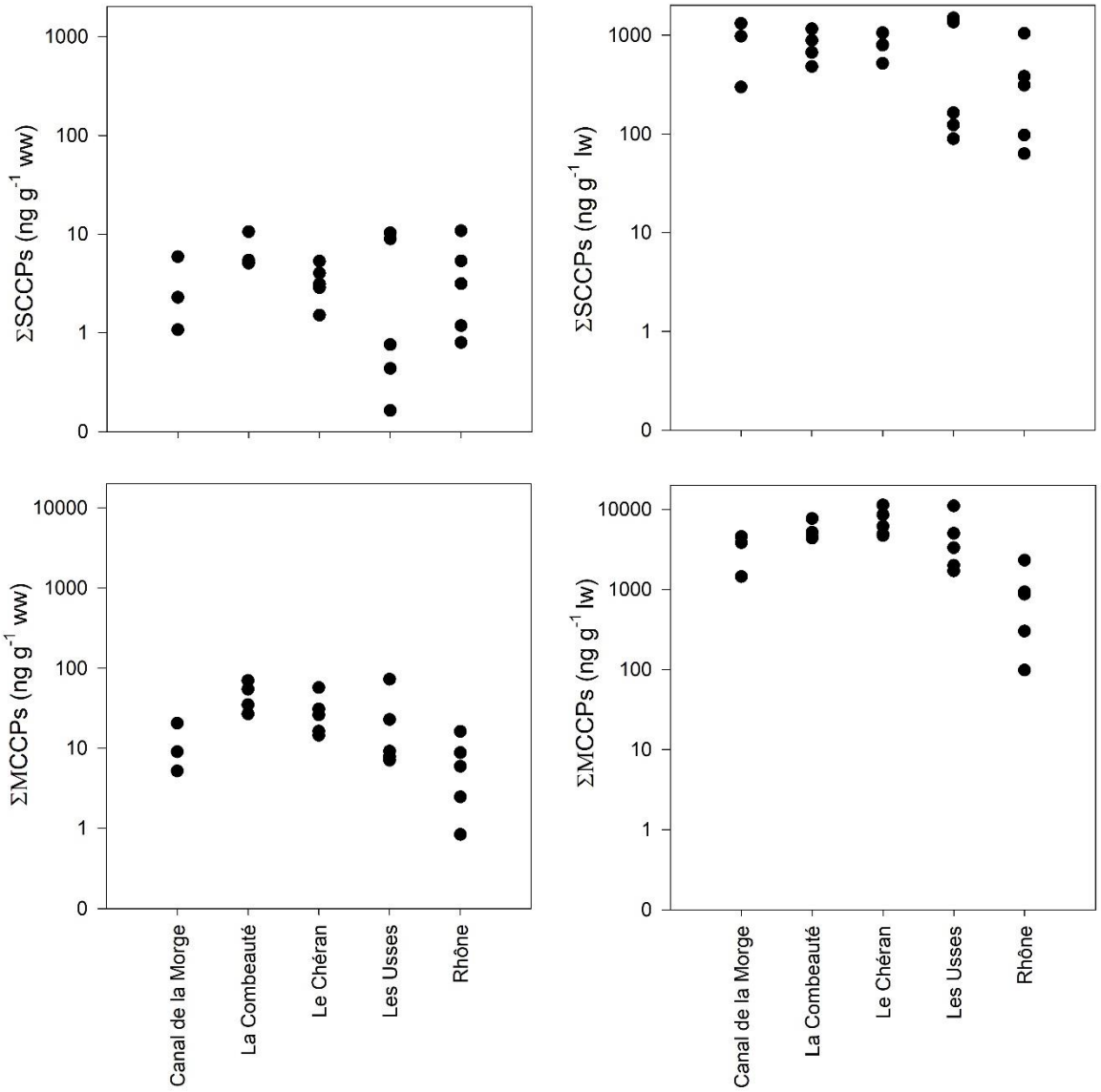

Figure 3. Total concentrations of SCCPs (top) and MCCPs (bottom) in individual common barbel collected from selected locations in the Rhône River watershed. ww: wet weight / lw: lipid weight

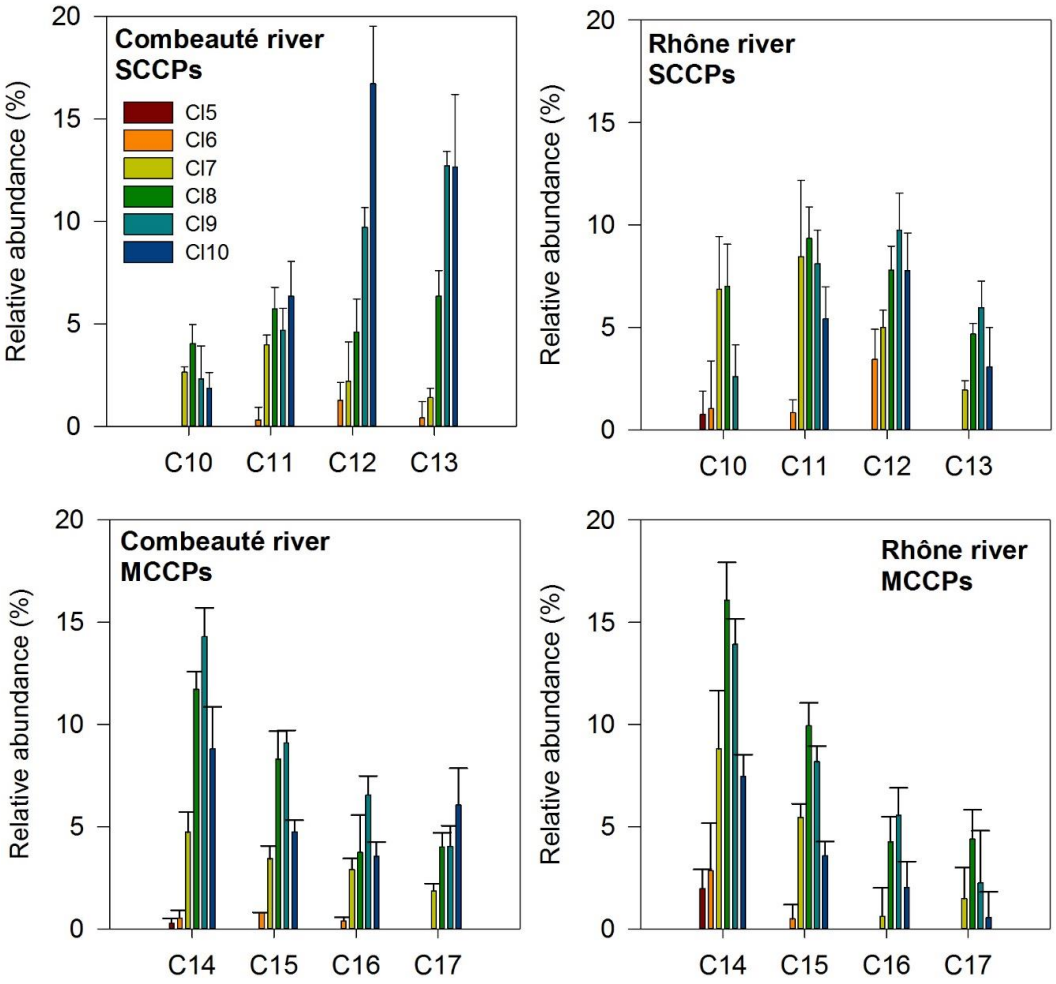

Figure 4. Average SCCP and MCCP congener group pattern in common barbel collected from the Combeauté River (left) and Rhône River (right). Error bars represent the standard deviation (n=4 and 5 for the Combeauté River and Rhône River, respectively).